Analysis and Modelling of Socket Termination for Wire Strand using Finite Element Methods

[1]Chunlei YU, [1]Wenguang JIANG*, [2]Lijuan YAN, [3]Jianying CUI, [3]Liping ZHU

[1]*School of Mechanical Engineering*, Yanshan University, Qinhuangdao, Hebei, 066004, China
[2]*Science, Technology and Quality Department*, Xuzhou Construction Machinery Group, Xuzhou, Jiangsu, 221004, China
[3]*Technology, Research and Development Center*, Juli Sling Co. Ltd, Baoding, Hebei, 072550, China

***Abstract* — A finite element model (FEM) for 7-wire strand with zinc alloy filled socket termination is developed in this paper. The domain superposition technique (DST) for efficient modelling of complex composite structures/materials has been used to implement the FEM. Full three dimensional solid model has been used in order to achieve accurate prediction. 8-noded brick elements were used throughout for structural discretization. Nonlinear effects including material plasticity, contact between wires, contact between the socket internal cone surface and the composite zinc alloy cone surface and friction between these contacting surfaces are all taken into account. Using the model developed, detailed mechanical behaviour of a realistic wire strand socket termination could be studied effectively.**

Keywords - wire strand; socket termination; finite element model; domain superposition technique; composite structure

I. INTRODUCTION

Socket termination is widely used for connecting wire rope and strand to other structural members. Compared to other types of clamping ends, it can provide high connection strength and stiffness, excellent stability and better resistance to corrosion and high temperature [1]. The use of socket termination to wire rope constitutes a wide class of important engineering components, called casting rigging.

Most of the published strand models are based on the hypothesis that the length of the strand is sufficiently long for the clamping conditions to be negligible [2-6]. However, the clamping conditions may be critical in determining the effective strand strength. Efficient and safe load transfer from the wire strand to the adjacent load-bearing element is a design requirement which demands at least as much attention as that of the load-bearing capacity of the strand itself. Owing to the complex geometry and loading of the socket termination, it is very difficult to establish an accurate analysis model. Dodd [7], Chaplin and Sharman [8], and Arend [9] studied the mechanism of load transfer between wires and casting material using analytical models which were all based on many simplifying assumptions. Utting and Jones [10,11] also recognized the termination effects but could not quantify it in detail. Chaplin and Bradon [12] developed a FEM for wire ropes with a resin filled socket termination. The load bearing capacity and the relative movement between the socket and the resin cone have been studied. In their model the wires within the resin cone were not modeled explicitly, instead an averaged equivalent material property was used to represent the wire-resin composite cone. Then Bradon and Ridge [13] compared the mechanical behaviour of socket terminations filled with white metal and resin respectively, using the same FEM as used in reference 12. Jiang and Henshall [14,15] analysed a 7-wire strand with rigidly fixed end using finite element (FE) method. Literature survey shows that a general and accurate model which could analyse the detailed mechanical behaviour of the socket termination for wire strand has not been found.

In this paper an accurate FEM for wire strand with zinc alloy filled socket termination has been developed to study the detailed mechanical behaviour. The conical wire grip is essentially a composite structure with a complex arrangement of reinforcement wire bundles bonded together by zinc alloy. It would be extremely difficult to build a quality FE mesh considering the detailed distributed narrow volume of zinc alloy material among the wires using traditional FE method. To overcome this difficulty, the DST proposed by the second author has been adopted [16,17], which was developed to deal with the difficulty faced when modelling composite materials with complex internal architectures. To make the strand model more accurate, the major nonlinear factors such as frictional contacts and material plasticity, which are difficult to deal with analytically, have all been taken into account in the model proposed in this paper.

II. FINITE ELEMENT MODEL

The configuration of the 7-wire strand with zinc alloy filled socket termination analysed is shown in Fig 1.

The strand consists of a straight center wire with radius R_1, surrounded by six helical wires with radius R_2. The geometry data of the strand is given in Table 1. The radius of the center wire is slightly larger than that of the helical wires, which ensures that contact occurs only between the center wire and each of the helical wires.

Iron serving wire was used to bind the strand to prevent wires from spreading out before casting. Its geometry is similar to a closely packed helical spring and the height in strand axial direction is about half of the strand diameter. The diameter of the iron wire is 0.8 mm.

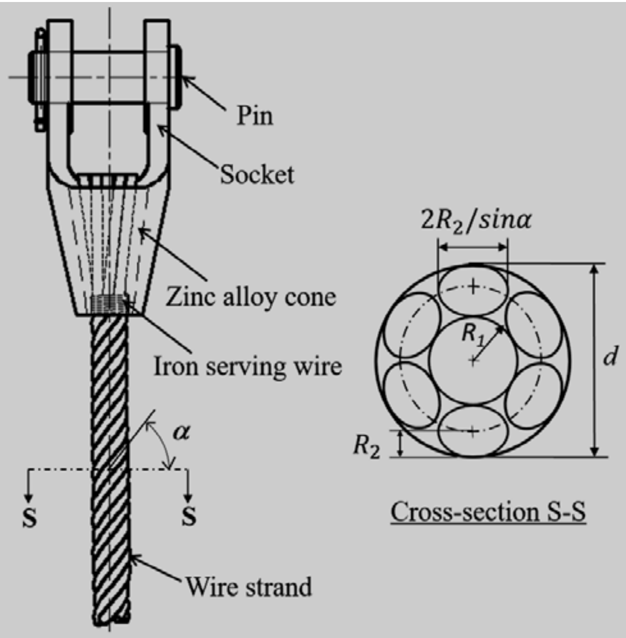

Figure 1. 7-wire strand with zinc alloy filled socket termination.

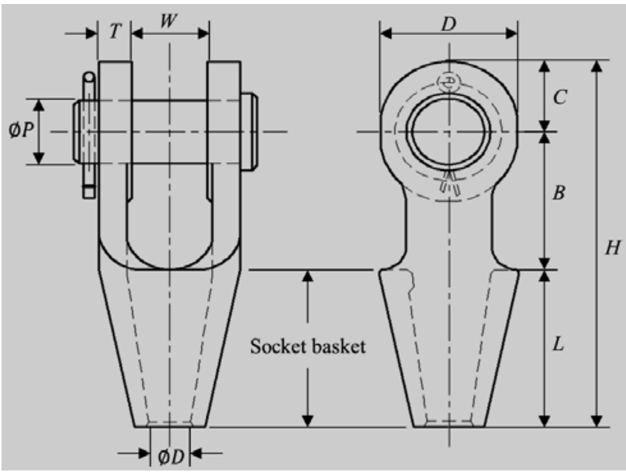

Figure 2. Typical open socket.

TABLE 1. GEOMETRY DATA OF 7-WIRE STRAND

Strand diameter d	11.4 mm
Center wire diameter $2R_1$	3.94 mm
Helical wire diameter $2R_2$	3.73 mm
Pitch length p	115 mm
Helical angle of the strand α	78.2°

Fig. 2 shows a typical open socket with a loading pin [18]. Its geometric parameters are given in Table 2.

TABLE 2. GEOMETRY DATA OF OPEN SOCKET (MM)

L	B	C	D	H	T	W	ϕD	ϕP
64	51	27	50	142	112	25	14	25

Fig. 3 shows the FE mesh of the 7-wire strand with zinc alloy filled socket termination. A commercial finite element analysis programme (ANSYS) was used throughout. Three dimensional 8-noded solid brick elements were used for structural discretization. This element is defined by eight nodes having three degrees of freedom at each node, i.e. translations in x, y and z directions. Contacts between the center and helical wires, and contact between the socket and the zinc alloy cone have been simulated using contact elements. They can simulate general surface-to-surface contact with Coulomb friction sliding.

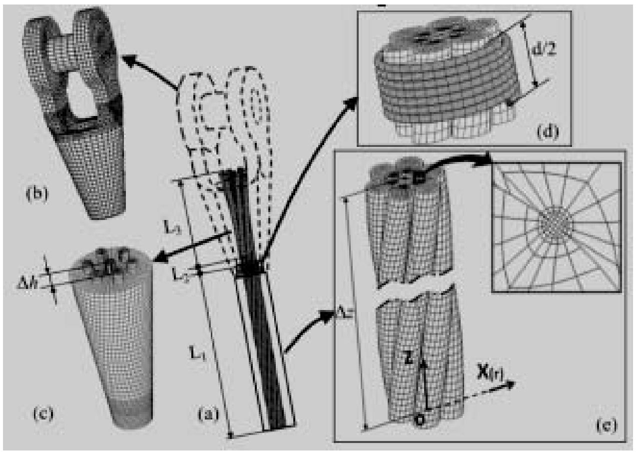

Figure 3. Finite element model of 7-wire strand with zinc alloy filled socket termination

Fig. 3(a) is the FE mesh for strand wires, which comprises three parts, i.e., the portion in L_1 with standard strand geometry, the middle portion in L_2 with a continuously varying helical angles increasing from α to the inner cone angle of the socket basket, and the third portion in L_3 with straighten-out helical wires. The length of the strand model outside the socket, Δz, should be long enough to ensure that the transition behaviour caused by the socket termination can be correctly simulated (Δz=103 mm in this paper). The length of the unlaid wires outside the socket, Δh, is 2 mm. Since the stresses vary rapidly in the vicinity of the wire contact lines, finer meshes were used in these local regions as shown in Fig 3(e). The FE mesh for the socket is shown in Fig 3(b).

The conical wire grip is essentially a composite structure with the equivalent reinforcement phase being the dispersed strand wires and the iron serving wire, and with the matrix bonding material phase being the cast zinc alloy, see Figs 3(c) and 3(d). The DST has been used to establish the conical wire grip composites simulation model. Only the separate FE meshes for every individual wires and the stand-alone meshed whole conical volume that the conical wire grip occupies without considering the complex reinforcement wires inside are needed. Therefore, the FE mesh for implementing DST is much easier to build and the meshing difficulty in coping with the degeneracy material volume when using the conventional FEM can be avoided. Using the highly automated implementation procedure developed, DST could assemble these separate meshes to form an integral mechanical model which can behaviour equivalently as the real conical wire grip does. For more detailed discussion about DST, interested readers are referred to Jiang et. al. [16] and Jiang [17].

The basic loading case of fixed end was applied to the FEM developed. For the socket end, an axial force was applied to the loading pin on the socket and proper non-rotation constraints were applied to the nodes on the center line of the pin. For the other end, i.e. the end free from end effects, the anti-symmetric and straight line deformation constraint relationships were applied to the nodal degrees of freedom, considering the symmetric features of the geometry and deformation. The detailed constraint equations can be referred to Jiang et al. [14].

The material properties for the wires [14], the zinc alloy [19], the socket [20], and the iron serving wire [20] are given in Table 3. Poisson's ratio for all material is 0.3. Coefficient of friction used for wire-wire contact is 0.115, and 0.2 for contact between zinc alloy cone and socket. The Von Mises yield criterion was assumed. A bilinear isotropic hardening material model has been used.

TABLE 3. MATERIAL PROPERTIES (GPA)

Material property	Wire	Zinc alloy	Socket	Iron wire
Young's modulus	188	83	201	201
Plastic modulus	24.60	4.15	4.045	4.806
Yield stress	1.54	0.26	0.835	0.195
Limit stress	1.80	0.33	0.98	0.375

III. FINITE ELEMENT ANALYSIS RESULTS AND DISCUSSION

Finite element analyses have been carried out using the model developed. An axial tension force was applied to the model at an increment of 5%F_0 and the maximum force applied was 95%F_0, where F_0 is the strand minimum breaking load and it can be calculated as follows [21]

$$F_0 = d^2 \sigma_b k / 1000 \qquad (1)$$

Where σ_b is the strand tensile strength, k is the coefficient, for the 7-wire strand k = 0.54, thus F_0=126 KN for the wire strand analysed in this paper.

When the axial tensile force is applied, the conical wire grip will be pulled into the conical recess in the socket. This will generate a wedging action that transfers the axial load between the strand and the socket. Owing to the helical nature of the structure, an induced axial twist moment will also generated in the strand.

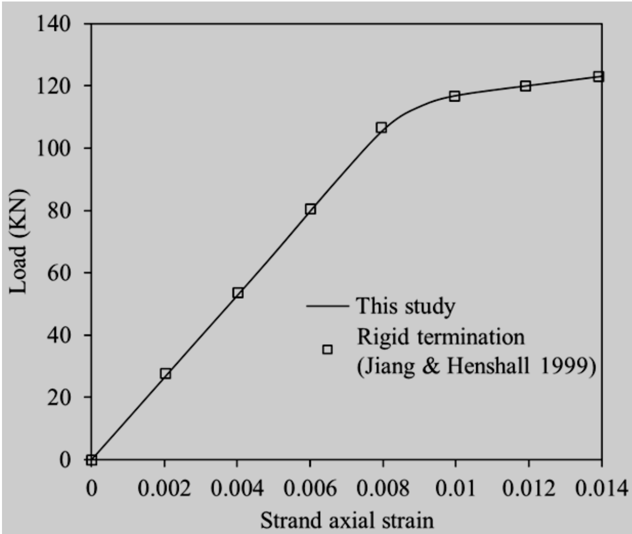

Figure 4. Variation of strand axial load with mean axial strain

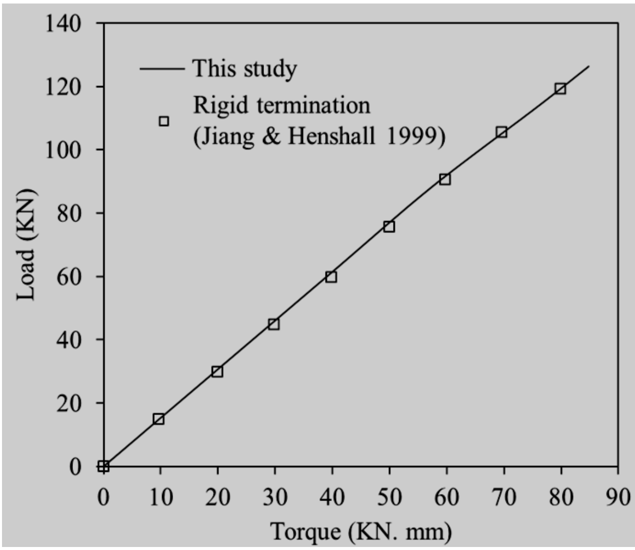

Figure 5. Variation of strand axial load with torque

Fig. 4 shows the strand axial load against mean strand axial strain extracted from the part of strand FE model outside the socket. Fig. 5 gives the variation of strand axial load with torque. The results have been compared with those obtained from the finite element model of Jiang et al. [14]. It can be seen that the two strand models yield the same strand

DOI 10.5013/ IJSSST.a.17.29.24

ISSN: 1473-804x online, 1473-8031 print

overall behaviour. These results indicate that the newly developed model can provide correct axial loading condition, i.e. both the axial force and the induced torque due to the helical geometric feature of the wire strand.

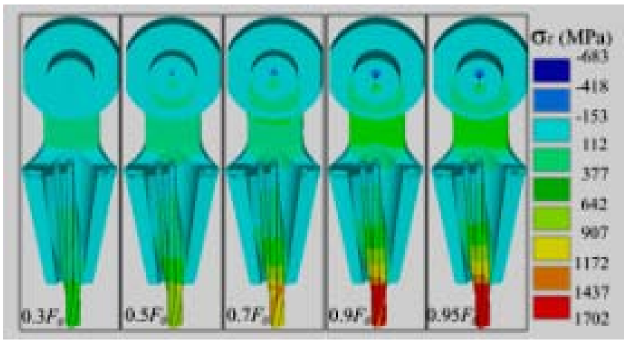

Figure 6. Axial stress distribution, σ_z, with varying axial load

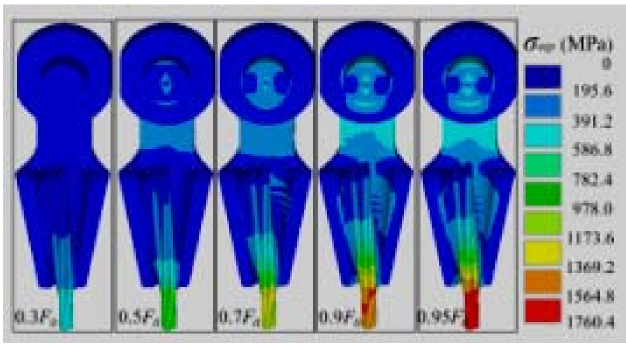

Figure 7. Von Mises equivalent stress distribution, σ_{eqv}, with varying axial load

Figs.6 and 7 present sample contour plots of the axial stress, σ_z, and the von Mises equivalent stress, σ_{eqv}, in partial model with varying axial load, respectively. From these two figures it can be seen that the axial stress is similar to that of the von Mises equivalent stress both in distribution pattern and magnitude. This indicates that the stress component in strand axial loading direction is predominant. For the reason of clear presentation, cutaway views are used in these figures, although the whole geometry has been modelled. This treatment also applies to the rest relevant figures.

Fig. 8 shows the variation of average wire axial stress along the length of the strand model for various loading levels. It can be seen from this figure that the axial stress in the center wire is higher than the stress in the helical wires. The constant stress region outside the socket, i.e. the length from 0 to 7d, is the region where the strand is free from termination influence. The immediate region just outside the socket with a length of about 2d is the termination influence region, within which the center wire axial stress slightly drops and the axial stress in helical wire slightly increases. After the strand wires enter inside the socket, the axial stresses in all wires drop very sharply first, and then gradually decrease to zero when the wires reach the end of the socket.

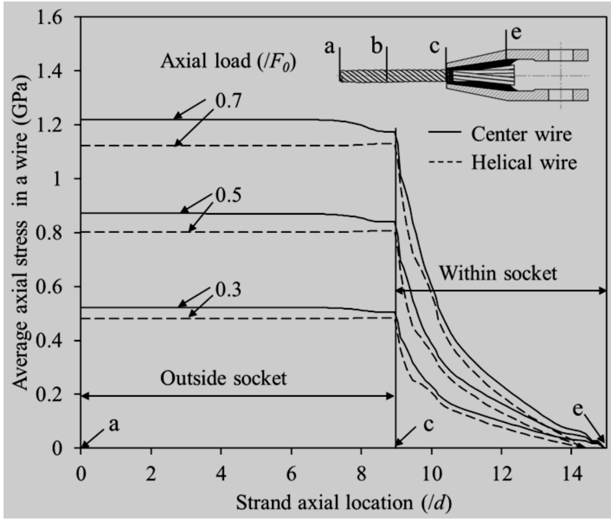

Figure 8. Variation of average axial stress along strand axial length

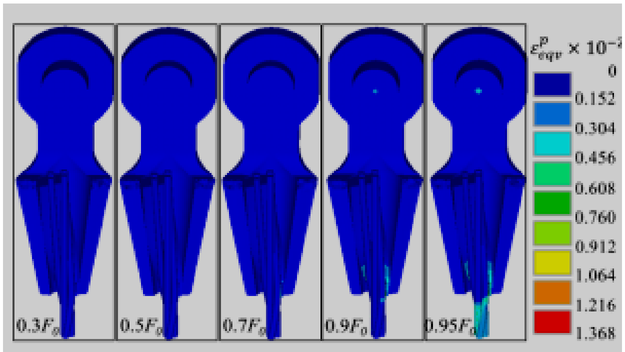

Figure 9. Distribution of equivalent plastic strain, ε^p_{eqv}, with varying axial load

Fig. 9 shows the distribution of equivalent plastic strain, ε^p_{eqv}, under the same load levels as those in Figs. 6 and 7. From this figure it can be seen that small plastic deformation region appears in the zinc alloy close to the socket small mouth at load level of about 50%F_0. When the strand load level reaches 95%F_0, we can observe that all strand wires outside the socket have experienced fully plastic yielding, but the zinc alloy material along only a quarter of the socket length has experienced plastic deformation. This means that the zinc alloy filled strand socket termination is strong enough to safely transfer the axial load that the strand itself can withstand.

Fig. 10 shows the variation of average contact pressure at the contact surfaces between the zinc alloy cone and the socket along the socket length. From this figure it can be seen that with the increase of strand axial load, the contact pressure also increases, as expected. The high contact pressure occurs at the socket small mouth where the serving wire locates and it decreases very sharply away from this point.

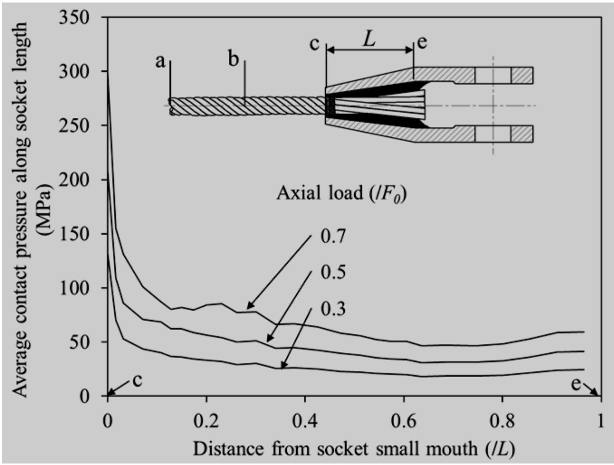

Figure 10. Variation of average contact pressure with distance from socket small mouth

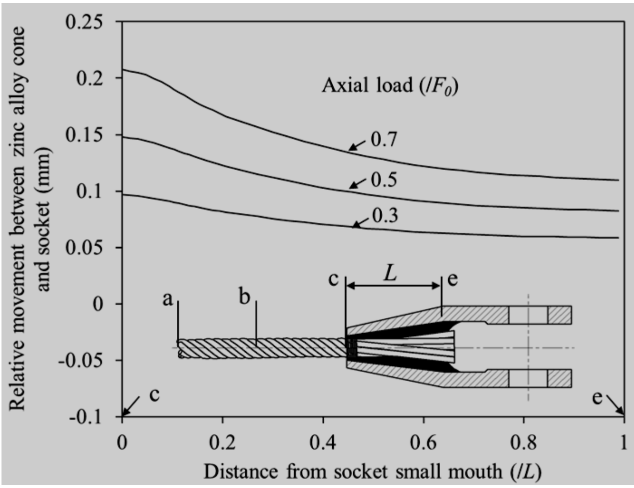

Figure 11. Variation of relative movement between zinc alloy cone and socket with distance from socket small mouth

Fig. 11 gives the variation of relative movement between the contact surfaces of the zinc alloy cone and the socket along the socket length. With increasing axial load, the relative movement increases. For a given axial load, the relative movement decreases with the distance from socket small mouth.

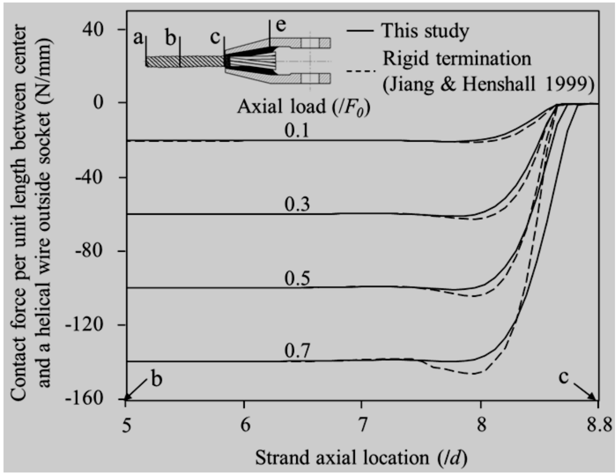

Figure 12. Variation of contact force per unit length of contact line along strand axial length outside socket

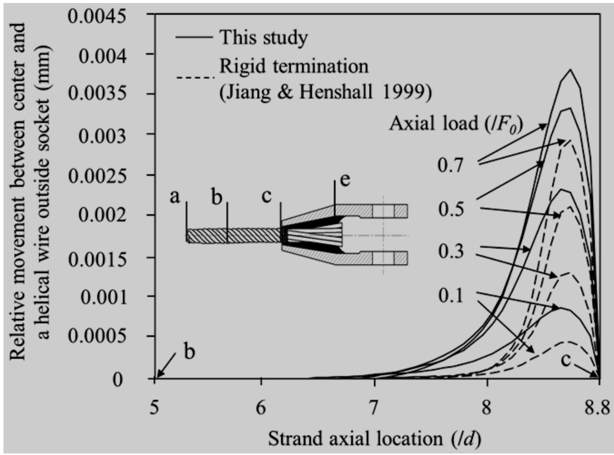

Figure 13. Variation of relative movement between contacting wires along strand axial length outside socket

To further investigate the socket termination effect outside the socket, Fig. 12 gives the distribution of contact force per unit length along contact lines between the core wire and the helical wires in the transition region just outside the socket. The result obtained from the present model has compared to that predicted by the model using a rigidly fixed end assumption [14]. The two models predict quite similar contact pressure distributions, except that the rigid end model predicted a slightly higher peak value.

Fig. 13 compares the distribution of relative movement along the contact line between the core wire and the helical wires in the same region as used in Fig. 12. Both the extent of the sliding region and the magnitude of the relative movement predicted by the present model are greater than those predicted from the rigidly fixed end model. Comparing Figs. 12 and 13, we can observe that there exist common regions where both active contact and relative sliding between contacting wire surfaces mutually occur. This indicates that, if strand axial load fluctuates, fretting fatigue in these regions may occur.

IV. CONCLUSIONS

A detailed finite element model for 7-wire strand with zinc alloy filled socket termination has been developed. The domain superposition technique has been used to establish the model of the conical wire grip composite structure. Both the time used for preparing the finite element mesh and the model size are greatly reduced. Using the model developed in this paper, the detailed complex behaviour of the widely used zinc alloy casting socket termination could be studied effectively. The numerical result shows that the casting termination structure is capable of bearing an axial load level as high as the breaking load of the wire strand itself without failure. For the specific socket termination structure analysed in the paper, the analysis results show that even when the strand is subject to very high tension load, the stress level within very large portion of the socket structure is still very low. This indicates that the current socket termination structural design could be very conservative.

ACKNOWLEDGMENTS

This work is funded by Hebei Provincial Natural Science Foundation, China (No. E2015203196).

REFERENCES

[1] I. Ridge and R. Hobbs, “The behavior of cast rope sockets at elevated temperatures,” Journal of Structural Fire Engineering, vol. 3, pp. 155-168, 2012.

[2] G. A. Costello, Theory of wire rope, 2nd ed. New York, Springer Verlag, 1997.

[3] W. G. Jiang, M. S. Yao and J. M. Walton, “A concise finite element model for simple wire rope strand,” International Journal of Mechanical Sciences, vol. 41, pp. 143-161, 1999.

[4] W. G. Jiang, J. L. Henshall and J. M. Walton, “A concise finite element model for three-layered straight wire rope strand,” International Journal of Mechanical Sciences, vol. 42, pp. 63-86, 2000.

[5] M. Raoof and I. Kraincanic, “Critical examination of various approaches used for analyzing helical cables,” Journal of Strain Analysis for Engineering Design, vol. 29, pp. 43-55, 1994.

[6] E. Stanova, G. Fedorko and S. Kmet, “Finite element analysis of spiral strands with different shapes subjected to axial loads,” Advances in Engineering Software, vol. 83, pp. 45-58, 2015.

[7] J. M. Dodd, “Resin as a socketing medium,” Wire Industry, vol. 15, pp. 343-344, 1981.

[8] C. R. Chaplin and P. C. Sharman, “Load transfer mechanics in resin socketed terminations,” Wire Industry, vol. 51, pp. 749-751, 1984.

[9] M. Arend, “The load transfer mechanicsms anchoring high-strength tension elements,” Proceedings of OIPEEC Round Table Conference Delft, vol. 3, September 1993.

[10] W. S. Utting and N. Jones, “The response of wire rope strands to axial tensile loads. 1. Experimental results and theoretical predictions,” International Journal of Mechanical Sciences, vol. 29, pp. 605-619, 1987.

[11] W. S. Utting and N. Jones, “The response of wire rope strands to axial tensile loads. 2. Comparison of experimental results and theoretical predictions,” International Journal of Mechanical Sciences, vol. 29, pp. 621-636, 1987.

[12] J. E. Bradon, C. R. Chaplin and I. M. L. Ridge, “Analysis of a resin socket termination for a wire rope,” Journal of Strain Analysis for Engineering Design, vol. 36, pp. 71-88, 2001.

[13] J. E. Bradon and I. M. L. Ridge, “Comparison of white metal and resin socket terminations for wire ropes,” Journal of Strain Analysis for Engineering Design, vol. 38, pp. 149-160, 2003.

[14] W. G. Jiang and J. L. Henshall, “The analysis of termination effects in wire strand using the finite element method,” Journal of Strain Analysis for Engineering Design, vol. 34, pp. 31-38, 1999.

[15] W. G. Jiang, “The development of the helically symmetric boundary condition in finite element analysis and its applications to spiral strands,” PhD Thesis, Brunel University, UK, 1999.

[16] W. G. Jiang, S. R. Hallett and M. R. Wisnom, “Development of Domain Superposition technique for the modelling of woven fabric composites,” Computational Methods in Applied Sciences, vol. 10, pp. 281-291, 2008.

[17] W. G. Jiang, “Implementation of domain superposition technique for the nonlinear analysis of composite materials,” Journal of Composite Materials, vol. 47, pp. 243-249, 2013.

[18] JuLi Co., Ltd. The Sling Products Handbook. Baoding: JuLi, 2015.

[19] E. Gervais, R. J. Barnhurst and C. A. Loong, “An analysis of selected properties of ZA alloy,” Journal of Metals, vol. 12, pp. 43-50, 1985.

[20] Z. M. Ceng, Mechanical Engineering materials manual, 7th ed. Beijing: China Machine Press, 2010.

[21] Z. Y. Pan and H. M. Qiu, The production process of wire rope. Hunan: Hunan University Press of Chinese, 2008.